Derivation of Oocytes from Mouse Embryonic Stem Cells

Karin Hübner,[1] Guy Fuhrmann,[3] Lane K. Christenson,[4] James Kehler,[1] Rolland Reinbold,[1] Rabindranath De La Fuente,[2] Jennifer Wood,[4] Jerome F. Strauss III,[4] Michele Boiani,[1] Hans R. Schöler[1]*

Continuation of mammalian species requires the formation and development of the sexually dimorphic germ cells. Cultured embryonic stem cells are generally considered pluripotent rather than totipotent because of the failure to detect germline cells under differentiating conditions. Here we show that mouse embryonic stem cells in culture can develop into oogonia that enter meiosis, recruit adjacent cells to form follicle-like structures, and later develop into blastocysts. Oogenesis in culture should contribute to various areas, including nuclear transfer and manipulation of the germ line, and advance studies on fertility treatment and germ and somatic cell interaction and differentiation.

In the early mammalian embryo, the germ line and soma are indistinguishable from each other. In the mouse, germ cell competence is induced at embryonic day 6.5 in proximal epiblast cells by signals emanating from the extraembryonic ectoderm (*1*, *2*). Even during the specification period, precursor cells give rise to primordial germ cells and certain somatic cells, such as extraembryonic mesoderm and allantois. The potential of embryonic stem (ES) cells to generate all lineages of the embryo in vivo has been widely reported in the literature, in striking contrast to the lack of data describing the derivation of germ cells from ES cells in vitro. We attributed the inability to demonstrate the derivation of germ cells from ES cells in culture to the lack of a suitable reporter system for the noninvasive visualization of germ cell formation.

Induction of germ cells in culture. Elucidation of the various known regulatory elements within the germline-specific gene

[1]Germline Development Group, [2]Female Germ Cell Biology Group, Center for Animal Transgenesis and Germ Cell Research, School of Veterinary Medicine, University of Pennsylvania, New Bolton Center, 382 West Street Road, Kennett Square, PA 19348, USA. [3]Centre de Neurochimie, Laboratoire de Neurobiologie du Développement et de la Régénération, FRE 2373 CNRS, 5 Rue Blaise Pascal, 67084 Strasbourg Cedex, France. [4]Center for Research on Reproduction and Women's Health, School of Medicine, University of Pennsylvania, 1349 Biomedical Research Building 2/3, 421 Curie Boulevard, Philadelphia, PA 19104, USA.

*To whom correspondence should be addressed. E-mail: Scholer@vet.upenn.edu

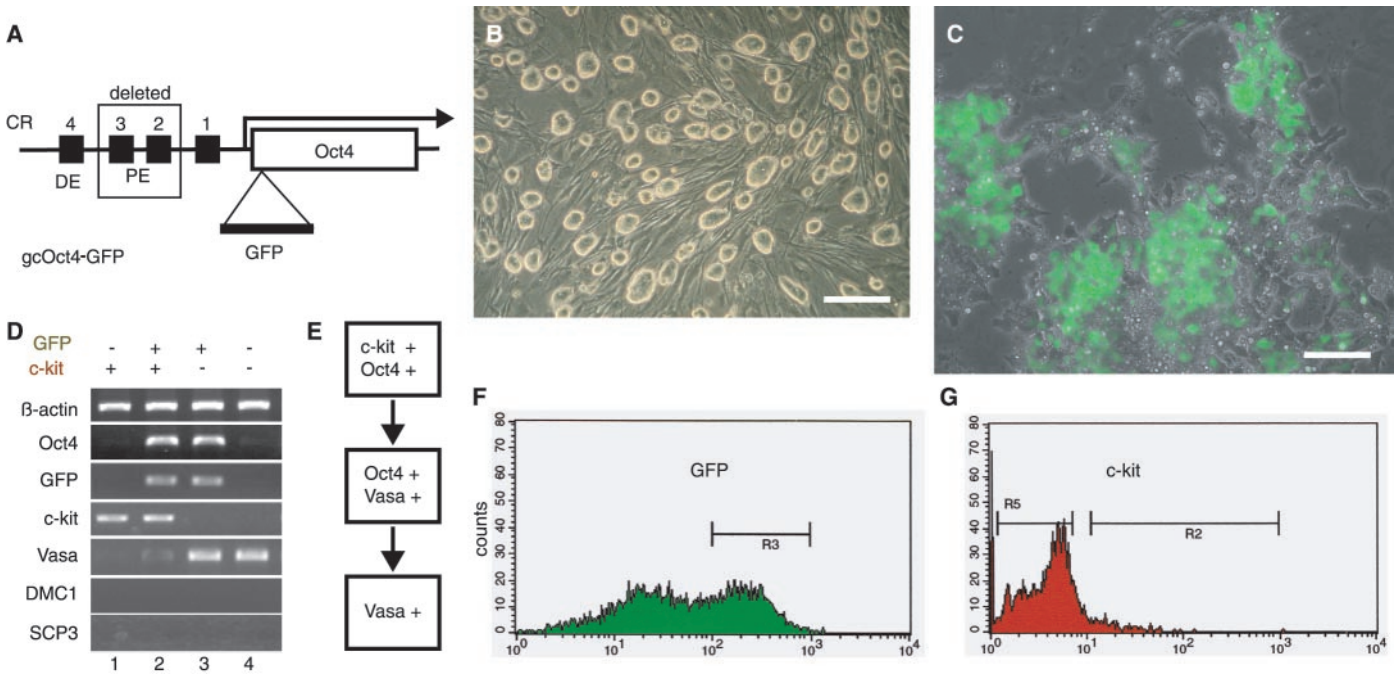

Fig. 1. Analysis of early stages of germ cell formation. (**A**) Schematic representation of the *Oct4* reporter gene (gcOct4-GFP) showing four conserved sequences (CR1 to 4) in the 5′ regulatory region with the deleted area boxed. The conserved sequences overlap with two regulatory elements: a distal enhancer (DE, germ cell–specific) and a proximal enhancer (PE, epiblast-specific) that have been described previously (*5*). (**B**) Phase contrast image of E14 ES cells transformed with gcOct4-GFP and growing on an embryonic fibroblast feeder layer (*42*). The clone presented here resulted in 3.5 dpc and 6.5 dpc mice embryos that lacked GFP expression but showed specific expression in germ cells of 12.5 dpc fetuses. (**C**) Merged fluorescent and phase contrast image of gcOct4-GFP ES cells 7 days (d7) after ~1 $\times 10^4$ to 2.5 $\times$ 10^4 cells/cm^2 were plated without feeder cells or growth factors in ES cell medium Bar scale for (B) and (C), 75 μm. (**D**) Expression analysis of four distinct cell populations of d7 cultures sorted by fluorescence-activated cell sorting (FACS) using markers GFP and c-kit. RT-PCR results for Oct4, the Oct4-GFP reporter, c-kit, Vasa, DMC1, SCP3, and β-actin are shown. (**E**) Scheme of differentiating early germ cells in vitro. Only positive markers are presented. (**F**) FACS analysis of a d9 culture using the gcOct4-GFP reporter. The R3 population was further sorted in (**G**) on the basis of c-kit staining, which shows that, at d9, only a minor fraction of gcOct4-GFP$^+$ cells are also positive for c-kit. R5 represents the population of c-kit negative cells, whereas R2 denotes cells in which c-kit is weakly or moderately expressed.

Oct4 (*3*, *4*) was instrumental in the development of a system that can visualize the initial steps of germ cell formation in vitro. Comparative analysis of the mouse, human, and bovine *Oct4* genes highlighted three conserved regions, CR2 to CR4, that lie within the known germ cell (DE) and epiblast (PE) enhancers (Fig. 1A) (*5*). To restrict expression of an Oct4-based reporter to germ cells during mouse development, we deleted CR2 and CR3 from a genomic Oct4 fragment driving an inserted green fluorescent protein (GFP) rather than Oct4 (*gcOct4-GFP*, Fig. 1A) (*6*). ES cells were transfected with *gcOct4-GFP*, and three positive clones were expanded and tested for specific expression in transgenic animals. Two transgenic lines showed specific *gcOct4-GFP* expression in germ cells and no signal in blastocysts or epiblast-stage embryos (*7*).

The same *gcOct4-GFP* ES cells (Fig. 1B) that had been used to generate transgenic mice were subsequently used to establish the conditions required to induce germ cell differentiation in vitro. ES cells were plated on tissue culture dishes and maintained in ES cell medium without any feeder cells or growth factors besides the factors present in the heat-inactivated serum. Expression of gcOct4-GFP was detected in some cells after 4 days (d4), in ~25% of all cells at d7 (Fig. 1C), and in 40% of all cells at d8 (not shown). Day 7 cultures were sorted into four cell populations on the basis of the levels of expression of the gcOct4-GFP reporter and endogenous c-kit, both being markers of early germ cells (Fig. 1D). After sorting, we further characterized cells by determining the mRNA expression of *Oct4*, *gcOct4-GFP*, *c-kit*, *Vasa* (a marker of postmigratory germ cells) (*8*), and two meiosis-specific markers, namely the synaptonemal complex protein 3 (*SCP3*) and the mouse homolog of the yeast meiosis-specific homologous recombination gene (*DMC1*) (*9*). The SCP3 protein is part of the axial-lateral element of the synaptonemal complex to which the chromatin loops are attached and is an excellent marker for detection of the meiotic transition in mammals because its expression is required for the onset of the first meiotic division (*10*). The DMC1 protein is supposed to function during chromosome synapsis and homologous recombination events (*11*, *12*).

Three of the sorted cell populations (GFP^+/c-kit^+, GFP^+/c-kit^-, and GFP^-/c-kit^-) contained cells at different stages of germ cell development (Fig. 1, D and E). The GFP^+/c-kit^+ fraction expressed *Oct4*, *gcOct4-GFP*, and *c-kit* but little *Vasa* mRNA (Fig. 1D, lane 2). Because *Vasa* is a marker for postmigratory germ cells until postmeiotic stages (*8*), these results suggest that these cells correspond to premigratory or migratory primordial germ cells. Cells sorted as GFP^+/c-kit^- (Fig. 1D, lane 3) were found to express *Oct4*, *gcOct4-GFP*, and *Vasa*, but not *c-kit*, and thus may represent cells of an early postmigratory germ cell stage. GFP^-/c-kit^- cells did not express *Oct4*, *gcOct4-GFP*, or *c-kit* mRNA but expressed *Vasa* mRNA (Fig. 1D, lane 4). These cells likely represent postmigratory germ cells that are about to enter meiotic prophase I, because these cells did not express the meiotic markers *DMC1* and *SCP3* (*9*). GFP^-/c-kit^- cells seem therefore to exhibit the same expression pattern as that in vivo, in which both *Oct4* and *c-kit* are downregulated in female germ cells before the zygotene-pachytene stage of meiotic prophase I, around 15.5 days postcoitum (dpc) (*13*). The fourth group (GFP^-/c-kit^+) was composed of cells that were not part of the germ line (Fig. 1D, lane 1) (*6*, *14*). Further analyses are required to define the identity of these c-kit^+ cells that 2 days later were almost absent (d9) (Fig. 1, F and G).

Early germ cell differentiation. In our cultures, colonies of variable size had formed by d12 (Fig. 2, A to C, represent a large colony). Large colonies in general exhibited reduced GFP expression but contained a high percentage of $Vasa^+$ cells (Fig. 2B). Within these colonies, three distinct types of cells were identified: (i) cells only expressing GFP, (ii) cells expressing both GFP and Vasa, and (iii) cells only expressing Vasa. Strings of GFP^+ and $Vasa^-$ cells were also found in the cultures, reminiscent of migratory germ cells (Fig. 2D) (*15*). GFP^+/$Vasa^+$ cells were always found in the vicinity of both GFP^+/$Vasa^-$ and GFP^-/$Vasa^+$ cells and may correspond to early postmigratory germ cells in vivo (Fig. 2B). GFP-expressing cells had nuclei with a more diffuse DNA staining, whereas cells solely expressing Vasa were more condensed, round, and physically separated from each other (Fig. 2A), which is typical of postmigratory germ cells. Outside the colonies, all cells were negative for germ cell markers and therefore most likely represent somatic cell types.

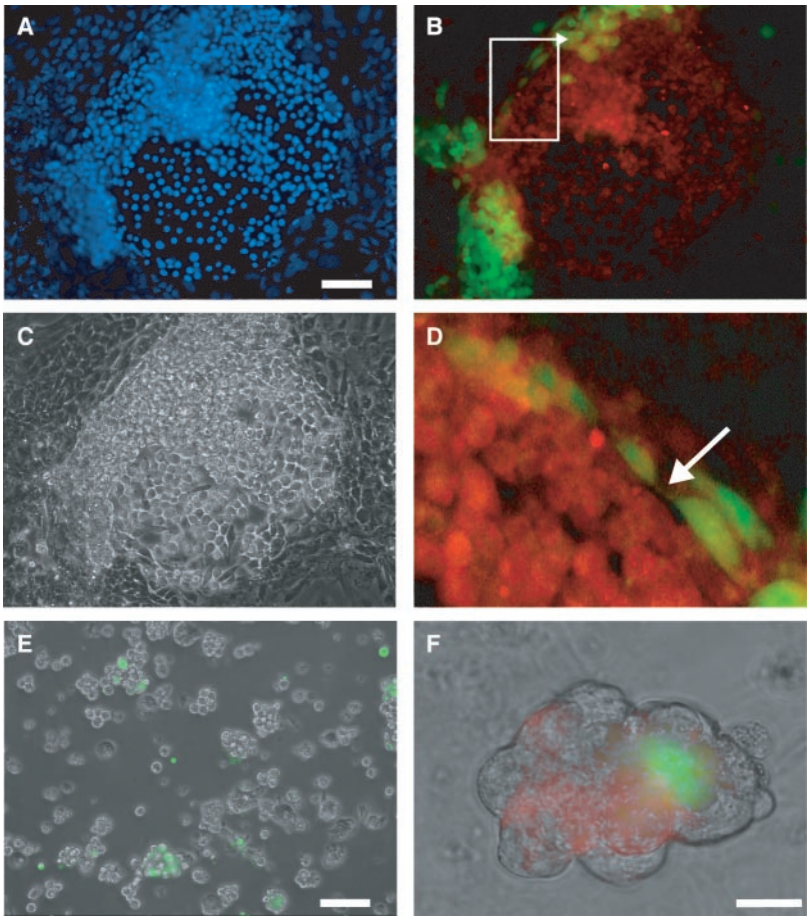

Fig. 2. Large d12 colony with different early germ cell stages. (**A**) Fluorescent image showing DNA localization (Hoechst staining, blue), (**B**) merged fluorescent image of gcOct4-GFP (green) and immunoreactive Vasa protein (red), and (**C**) phase contrast image. Boxed area in (B) is enlarged in (**D**) to show a string of gcOct4-GFP^+ cells (arrow). (**E**) Merged fluorescent GFP and phase contrast image of the supernatant from a d12.5 culture. (**F**) Merged fluorescent (green, GFP; red, Vasa) and phase contrast image of one aggregate with a single GFP^+ cell. All pictures represent whole mount stainings. Bar scales, 50 μm in (A) to (C) and (E) and 25 μm in (F).

Individual cells or groups of cells detached simultaneously from the large colonies, but in both cases these predominantly Vasa$^+$ germ cells tended to form small aggregates in the supernatant, with very few GFP$^+$ cells (Fig. 2, E and F). It is likely that these cells detach because of the loss of cell-cell contacts, as noted in the lower center area of the colony (Fig. 2, A to C). A reduction in cell-cell adhesion among these Vasa$^+$ germ cells in culture is quite similar to that of postmigratory germ cells in vivo (*8*). Interestingly, the aggregates were frequently attached to GFP$^-$/Vasa$^-$ cells, which often resulted in a more compact structure than that within the original colony (Fig. 2F). These tightly knit structures are quite similar to the histotypic structures obtained after disaggregation by mild trypsin treatment of male or female genital ridges (*16*, *17*). Furthermore, cultures of suspended ovarian cells of newborn mice and rat can also yield primordial follicles (*18*).

Formation of follicular structures. Aggregates were collected by centrifugation and cultured in new plates. Well-organized structures formed, and some of these were morphologically similar to early ovarian follicles (Fig. 3, B and C) (*6*). During the next 2 weeks, advanced follicle-like structures formed both in the master plate and aggregate cultures (Fig. 3, E, F, and H). The majority of these structures degenerated upon further cultivation, and ~20% produced oocytes larger than 40 μm.

In the mammalian female gonad, the development of a meiotically competent oocyte requires the interaction of somatic cells, which work in cooperation to synthesize estradiol. Androgen precursors produced by theca cells are aromatized into estrogen by granulosa cells. Detection of estradiol in our cultures, therefore, provides evidence for functional activity of the somatic cells in these follicle-like structures. We consistently found estradiol in the culture medium by d12, with levels peaking around d20. Thereafter, estradiol levels decreased (Fig. 3A). To determine whether estradiol production was associated with expression of steroidogenic enzymes, we performed quantitative reverse transcription polymerase chain reaction (RT-PCR) for key genes involved in estrogen biosynthesis, including *steroidogenic acute regulatory protein* (*StAR*), *P450 17α-hydroxylase-17/20 lyase* (*CYP17*), and *P450 aromatase* (Fig. 3G) (*19*). The mRNAs of *P450 aromatase*, *CYP17*, and *StAR* were 4.3-, 3.3-, and 1.8-fold greater, respectively, in d22 attached cultures compared with those at d16. Increased expression of these genes correlated with the observed increased concentration of estradiol in the medium. The steroidogenic gene expression profiles for attached cells at d16 were compared with those of replated cells at d16F 4 days after replating. This comparison illustrated pronounced differences between the two cell populations, including increased expression of *P450 aromatase* (2.4-fold), *CYP17* (1.4-fold), and *StAR* (3.5-fold) in d16F cells. These higher levels are likely the result of an increased proportion of follicular to nonfollicular somatic cells in the replated culture. This is also supported by the sevenfold increase in growth differentiation factor (*GDF-9*) in the replated cells as compared with attached cells (d16 and d16F, Fig. 3D). Increased expression of the oocyte-specific cell marker *GDF-9* in the replated cultures is an interesting phenomenon, because this growth factor is required for ovarian folliculogenesis (*20*, *21*). The expression of steroidogenic enzymes and follicular estrogen synthesis is typically thought to require gonadotropin support. However, expression of steroidogenic enzymes may occur in the absence of gonadotropins, because transfection of ES cells with steroidogenic factor–1 (SF-1), for example, induces steroidogenic enzyme expression (*22*). In addition, the serum and possibly endogenously produced gonadotropins in the cultures may provide sufficient hormonal support.

Characterization of oocytes. As early as d26 of culture, oocyte-like cells were released from the vicinity of their companion somatic cells (Fig. 3I) and found floating in the supernatant. The oocyte-like cells were enclosed in a coat resembling the zona pel-

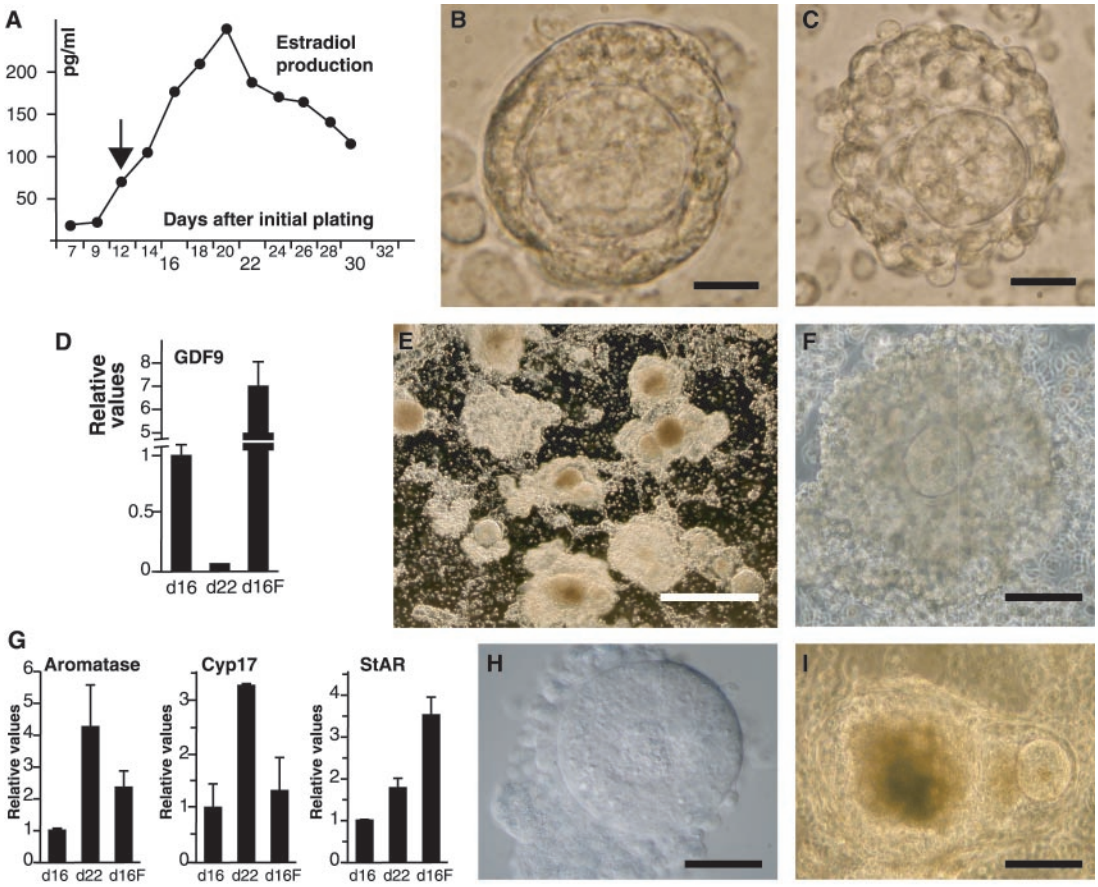

Fig. 3. Formation and characterization of follicle-like structures. (**A**) Media estradiol levels (pg/ml) from cultures between d7 and d34. (**B** and **C**) Representative phase contrast images of structures that are morphologically similar to early primary or secondary follicles. (**D**) Quantitative RT-PCR analysis of *GDF-9* in d16 and d22 cultures and in d16F-replated cultures. (**E**), (**F**), and (**H**) depict aggregate cultures and show that many of the follicle-like structures maintain their three-dimensional organization. (F) is a magnified representation of (E) at a different area of the same culture. (I) represents an adherent culture; all other panels show nonadherent cells and structures. (**G**) Quantitative RT-PCR analysis of *aromatase*, *CYP17*, and *StAR* in d16 and d22 cultures and in d16F-replated cultures. (**I**) Phase contrast image of oocyte-like cells released from d26 culture. All pictures are whole mount stainings. Bar scales: 15 μm in (B), 30 μm in (C), 500 μm in (E), 50 μm in (F), 40 μm in (H), and 100 μm in (I).

lucida, which was fragile and easily lost when manipulated with a micropipette (compare Fig. 4, B and C). Most of these cells were 50 to 70 μm in size, which is in the size range of natural oocytes (*23*). However, some looked swollen, reaching a size of 130 μm, and had a thinned zona (Fig. 4C). They were GFP^+, in accordance with Oct4 being reexpressed after birth in diplotene-arrested oocytes (Fig. 4D) (*13*). The large cells also exhibited cytoplasmic staining for zona pellucida proteins 2 and 3 (ZP2 and ZP3, respectively) (*24*) at a location predominantly adjacent to or in the cell membrane, which is distinct from that of the GFP signal (Fig. 4E, ZP2 shown in red; ZP3 not shown). To support the immunocytochemical analysis, we examined the cultures for mRNA expression of several oocyte-specific markers, including *ZP1*, *ZP2*, *ZP3*, a factor in the germ line (*Figα*), and *GDF-9* (*20*, *21*, *24–27*). Figα, a transcription factor required for the expression of *ZP1*, *ZP2*, and *ZP3*, was absent in the ES control cells (not shown) and expressed at similar levels between d16 and d30 (Fig. 4A). As expected, expression of both *ZP2* and *ZP3* was also observed; however, *ZP1* expression was not detectable (Fig. 4A, lanes 2 to 4). This may indicate that factors required for specific expression of *ZP1* are not properly expressed in our cultures. Because ZP1 serves as a linker for ZP2 and ZP3 (*28*), its absence may account for the fragile zona observed on the ES-derived oocytes. Loss of ZP1 has been reported to perturb but not impair folliculogenesis (*28*).

Expression of the murine oocyte-specific *GDF-9* in the d16 and d22 adherent cultures and the increase in *GDF-9* mRNA levels in the replated aggregate cultures (d16F; with a high oocyte/somatic cell ratio) provide additional evidence for folliculogenesis (Fig. 3D). Loss of *GDF-9* expression (15.2-fold decrease) between d16 and d22 in the adherent cultures is also consistent with loss of oocyte *GDF-9* expression as follicular growth occurs (*20*).

Evidence of meiosis. *DMC1* expression and lack of *SCP3* expression as determined by RT-PCR at d16 indicated that the ES-derived germ cells were about to enter meiosis (*6*). To further substantiate entry into meiosis, we mildly disaggregated d16 cultures with trypsin, replated them, and collected single cells of varying sizes after the majority of the cell population had reattached (Fig. 5A). Expression and distribution of SCP3/COR1 (Fig. 5, B, D, F, and I) or SCP1/SYN1 (not shown) within these cells were analyzed with the use of the respective antibodies (*29*, *30*). Germ cells indistinguishable in size from somatic cells showed SCP3/COR1 staining (Fig. 5, A, white arrows, and B) that was very similar to that of female germ cells isolated from day 15.5 embryos (Fig. 5C), suggesting that these cells are in a stage before leptotene. Germ cells up to 25 μm in size showed SCP3/COR1 staining that colocalized with the nucleus (Fig. 5, A, black-white arrow, and D to F). In contrast, SCP3/COR1 was undetectable in accompanying smaller cells (Fig. 5, D to F) or in germ cell controls in which the primary antibody had been omitted (not shown). In large germ cells (Fig. 5A, black arrow), SCP3/COR1 (Fig. 5, G to I) and SCP1/SYN1 (not shown) were localized predominantly in the cytoplasm, which is indicative of a more advanced meiotic stage (*28*). Addition of gonadotropins, i.e., pregnant mare serum gonadotropin and human chorionic gonadotro-

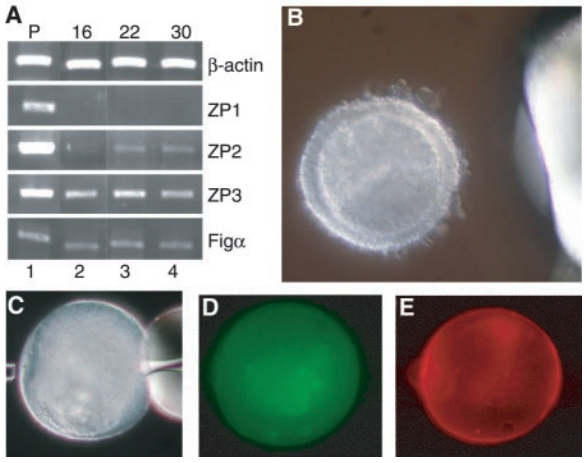

Fig. 4. Characterization of oocytes. (**A**) RT-PCR analysis of cultures at three different time points, compared with an ovarian newborn tissue control (*P*). Comparison of expression levels of oocyte-specific markers *ZP1*, *ZP2*, *ZP3*, and *Figα* by RT-PCR shows that at d30 only *ZP1* remains absent. β-*actin* served as an internal standard. (**B**) Phase contrast image of a small oocyte-like cell with holding pipette (right). (**C**) Phase contrast image of grown oocyte-like cell with holding pipette (right) and injection needle (left) for size comparison. (**D**) Fluorescence image of gcOct4-GFP, and (**E**) ZP2 immunostaining of the same cell shown in (C).

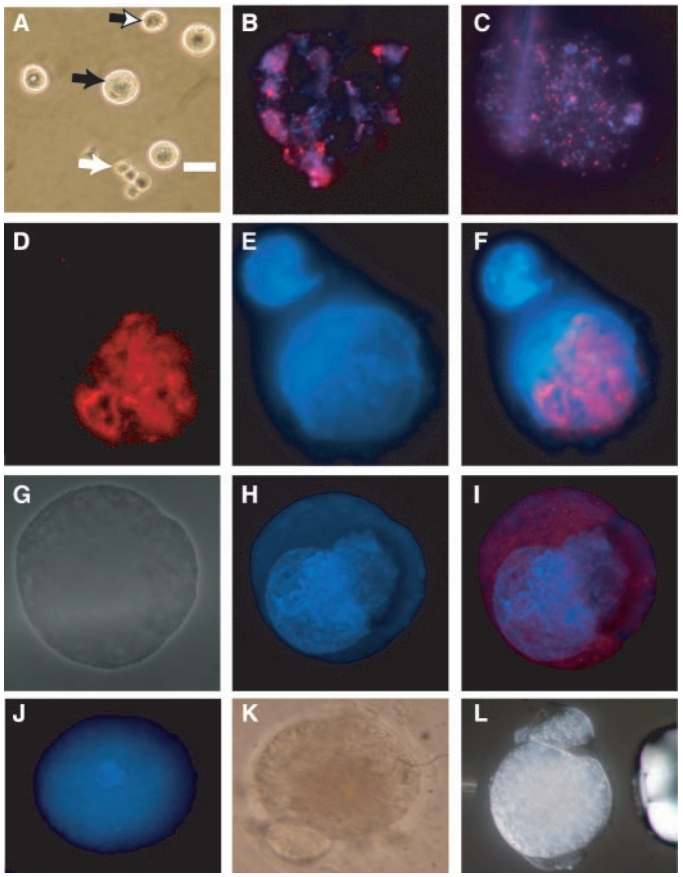

Fig. 5. Germ cells showing meiotic markers. (**A**) Image of putative germ cells selected from cultures on the basis of size of cells. The white arrow marks a cell that is representative for the size of cells stained in (B) and (C); the black-white arrow, cells representative for (D) to (F); the black arrow, germ cells representative for (G) to (I). Bar scale, 25 μm. (**B**) SCP3 staining of a germ cell derived from ES cell cultures in comparison with a germ cell derived from a day 15.5 embryonal ovary. (**C**) The highly decondensed chromatin appearance suggests that the cell in (B) is in a preleptotene stage. (**D** to **F**) represent a germ cell showing nuclear SCP3 staining (D). (**G** to **I**) illustrate a germ cell that has progressed to a diplotene-like nuclear configuration. (**J**) Chromatin condensation surrounding the nucleolus in large oocyte-like cells. Images of oocyte-like cell directly after hormone-induced extrusion from follicle (**K**) and after fixation (**L**) showing a structure resembling the polar body within the zona. (A), (G), (K), and (L) are phase contrast images; (D) is a fluorescent image for SCP3/COR1 protein (red); (E), (H), and (J) are stained for DNA (blue); (B), (C), (F), and (I) are merged fluorescent images showing SCP3/COR1 protein in relationship to DNA.

pin, to isolated follicles resulted in extrusion of oocytes and formation of a structure that morphologically resembles a polar body, suggesting that some oocytes in the cultures can complete the first phase of meiosis (Fig. 5, J, K, and L).

Blastocyst-like structures derived from ES cells. At about d43, structures are found in the cultures that, with respect to morphology (Fig. 6, A to M) and expression of molecular markers (Fig. 6, M and N), are similar to mouse preimplantation embryos. A defined zona around the embryo was only detected in a few cases (for example, Fig. 6B), which is likely a consequence of its fragile structure. A zona was identified after it had detached from the embryo (compare Fig. 6, C and D, showing the same embryo on 2 subsequent days). This embryo had defined features of a 16-cell morula (Fig. 6, E to G). Nuclear staining by Hoechst, the cytoplasmic-to-nuclear ratio, a compacted morphology, and Oct4 protein expression and distribution, which at this stage starts to be localized predominantly to the nucleus [Fig. 5C in (*31*)], are characteristic for a mouse morula. Several structures were found in our cultures that resembled blastocysts (Fig. 6, H to L, show a representative collection of five different blastocyst-like structures).

It is likely that the structures resembling preimplantation embryos represent parthenotes, as suggested by the similarity of our follicle outgrowths (Fig. 6A) to parthenogenetically activated oocytes of the LT/Sv mouse strain (*32*). Future experiments will address whether cleavage was induced by the culture conditions. It is well known that agents such as ethanol or cations or thermic shock of the oocytes during the observations may induce parthenogenesis with or without extrusion of a second polar body. Addressing these and related questions may provide a better understanding of the physiological problems of parthenogenesis in vivo. In addition, our system may contribute to a better understanding of the regulation of spontaneous ovarian teratocarcinogenesis and the molecular mechanism by which genes such as *c-mos* block the second meiotic metaphase arrest (*22*, *33*, *34*).

Summary and conclusions. It is not surprising that the derivation of oocytes and blastocyst-like structures could be accomplished with both female and male ES cells. In the absence of appropriate *SRY* expression in the gonads, male primordial germ cells enter the female pathway and often undergo the first step of oogenesis, entering meiotic arrest at prophase I [for review see (*35*)]. Male-to-female sex reversal even happens in the mammalian embryo when single genes such as *Sry*, *Sox9*, or *Fgf9* are not properly regulated or deleted (*36*). Because we detected *Sry* expression by RT-PCR only in the later stages of our cell cultures (not shown), the gene may not be efficiently regulated in the areas where germ cells differentiated into female germ cells.

The reports from 1978 cited above in the context of dissociation and reaggregation of gonadal cells are interesting also in this con-

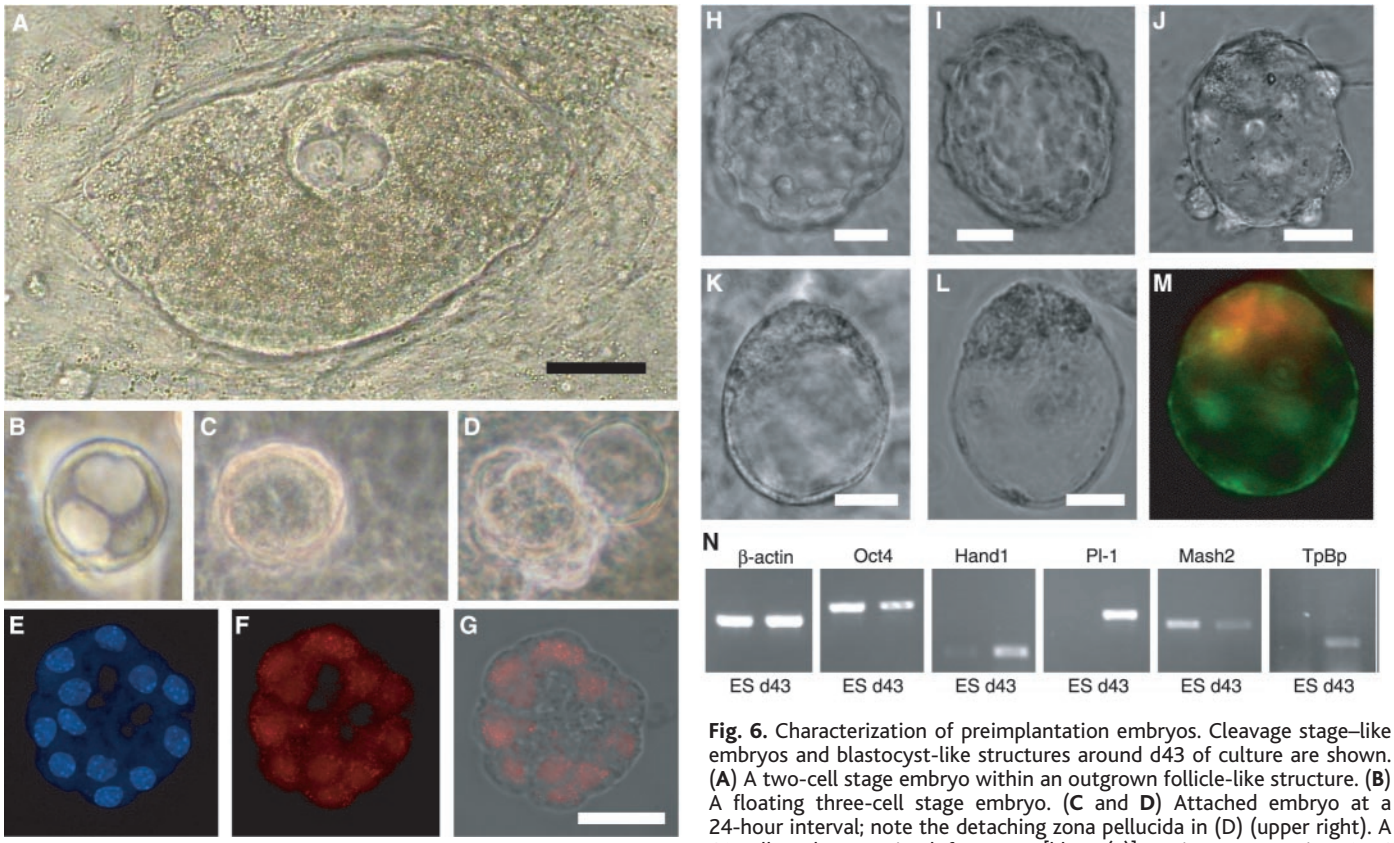

Fig. 6. Characterization of preimplantation embryos. Cleavage stage–like embryos and blastocyst-like structures around d43 of culture are shown. (**A**) A two-cell stage embryo within an outgrown follicle-like structure. (**B**) A floating three-cell stage embryo. (**C** and **D**) Attached embryo at a 24-hour interval; note the detaching zona pellucida in (D) (upper right). A 16-cell embryo stained for DNA [blue, (**E**)] or immunoreactive Oct4 protein [red fluorescence, (**F**)]; (**G**) is a merged phase contrast and Oct4 protein image. Four blastomeres were removed before fixation [see holes in (F)]. (**H**) Blastocyst-like embryo with reduced cell-cell contact within the structure. (**I** and **J**) Blastocysts lacking a characteristic flattened outer trophoblast cell layer, instead nuclei bulge out. This appearance is also found in natural blastocysts when the zona pellucida is removed before cleavage of the embryo (not shown). (**K** and **L**) Two blastocyst-like structures that are morphologically indistinguishable from natural blastocysts. (**M**) Immunocytochemical localization of Troma-1 to the outer layer of cells (green) and Oct4 protein (red) to inner cells that are acentrically located in the blastocyst-like structure, a staining pattern typical of natural blastocysts. (A) to (D) and (H) to (L) are phase contrast images; (M) is a merged fluorescent image of the embryo shown in (L). (**N**) RT-PCR analysis of d43 cultures and ES cells under nondifferentiating conditions shows differential expression of *Hand1*, *Pl-1*, and *TpBp* in reference to β-*actin* expression. *Oct4* is expressed in both samples, which reflects the critical role of Oct4 in the inner cell mass of blastocysts and in ES cells. *Mash2*, although essential for extraembryonic development (*42*), is also expressed in ES cells. Bar scales: 100 μm in (A), 40 μm in (G), 30 μm in (H), 25 μm in (I), 45 μm in (J), 30 μm in (K), and 20 μm in (L).

text (*16*, *17*). Disintegration and reaggregation of male mouse and rat testes resulted in long, twisting tubular structures as well as spherical aggregates (*16*, *17*). One type of aggregate was indistinguishable in appearance from isolated medium-sized ovarian follicles in suspension and thus termed "folliculoids." The yield of folliculoids in these cultures was markedly increased when treated with antibodies specific for H-Y, an antigen that is responsible for the differentiation of the undetermined gonadal anlage into a testis [for review see (*37*)]. Because even cells of natural gonads form such "folliculoids," the formation of similar structures from male ES cells seems not too farfetched to us.

Two main arguments have been put forth to explain why ES cells are not totipotent in vitro. Mouse ES cells have not been observed to give rise to germ cells in vitro, nor have they been shown to differentiate along the trophectodermal lineage. Expression of trophectodermal markers, like Troma-1 protein (Fig. 6M) or *Pl-1*, *Hand-1*, and *TpBp* mRNAs (Fig. 6L) (*38*–*40*), together with the morphology of the structures observed, strongly suggests that a trophoblast is formed from ES cells in vitro. Notably, our blastocyst-like structures looked better than most of those obtained by nuclear transfer of somatic nuclei. In addition, they had the correct *Oct4* expression, which is in contrast to most clones, and yet the latter are generally considered to represent blastocysts (*41*). We conclude that mouse ES cells are capable of differentiating into oocytes and form structures very similar, if not identical, to blastocysts, thereby demonstrating that these cells are actually totipotent even in vitro. Future experiments will reveal whether the oocytes we have generated in culture from ES cells can be fertilized, whether they have undergone a gender-specific resetting of the epigenetic marks (imprinting), and whether they can be used as starting material to derive ES cell lines after nuclear transfer.

References and Notes

1. K. A. Lawson, W. J. Hage, *Ciba Found. Symp.* **182**, 68 (1994).
2. K. A. Lawson *et al.*, *Genes Dev.* **13**, 424 (1999).
3. M. Pesce, M. K. Gross, H. R. Schöler, *Bioessays* **20**, 722 (1998).
4. M. Pesce, H. R. Schöler, *Mol. Reprod. Dev.* **55**, 452 (2000).
5. V. Nordhoff *et al.*, *Mamm. Genome* **12**, 309 (2001).
6. Materials and methods are available as supporting material on *Science* Online.
7. K. Hübner *et al.*, in preparation.
8. Y. Toyooka *et al.*, *Mech. Dev.* **93**, 139 (2000).
9. S. Chuma, N. Nakatsuji, *Dev. Biol.* **229**, 468 (2001).
10. L. Yuan *et al.*, *Mol. Cell* **5**, 73 (2000).
11. K. Yoshida *et al.*, *Mol. Cell* **1**, 707 (1998).
12. D. L. Pittman *et al.*, *Mol. Cell* **1**, 697 (1998).
13. M. Pesce, X. Wang, D. J. Wolgemuth, H. Schöler, *Mech. Dev.* **71**, 89 (1998).
14. M. Saitou, S. C. Barton, M. A. Surani, *Nature* **418**, 293 (2002).
15. R. Anderson, T. K. Copeland, H. Schöler, J. Heasman, C. Wylie, *Mech. Dev.* **91**, 61 (2000).
16. M. T. Zenzes, U. Wolf, E. Gunther, W. Engel, *Cytogenet. Cell Genet.* **20**, 365 (1978).
17. S. Ohno, Y. Nagai, S. Ciccarese, *Cytogenet. Cell Genet.* **20**, 351 (1978).
18. A. McLaren, D. Southee, *Dev. Biol.* **187**, 107 (1997).
19. L. K. Christenson, R. L. Stouffer, J. F. Strauss 3rd, *J. Biol. Chem.* **276**, 27392 (2001).
20. J. Dong *et al.*, *Nature* **383**, 531 (1996).
21. M. M. Matzuk, *Mol. Cell. Endocrinol.* **163**, 61 (2000).
22. P. A. Crawford, Y. Sadovsky, J. Milbrandt, *Mol. Cell. Biol.* **17**, 3997 (1997).
23. J. J. Eppig, M. J. O'Brien, *Biol. Reprod.* **54**, 197 (1996).
24. I. J. East, D. R. Mattison, J. Dean, *Dev. Biol.* **104**, 49 (1984).
25. O. Epifano, L. F. Liang, M. Familari, M. C. Moos Jr., J. Dean, *Development* **121**, 1947 (1995).
26. S. M. Soyal, A. Amleh, J. Dean, *Development* **127**, 4645 (2000).
27. L. Liang, S. M. Soyal, J. Dean, *Development* **124**, 4939 (1997).
28. T. Rankin, P. Talbot, E. Lee, J. Dean, *Development* **126**, 3847 (1999).
29. M. Tarsounas, R. E. Pearlman, P. B. Moens, *J. Cell Sci.* **112**, 423 (1999).
30. M. J. Dobson, R. E. Pearlman, A. Karaiskakis, B. Spyropoulos, P. B. Moens, *J. Cell Sci.* **107**, 2749 (1994).
31. S. L. Palmieri, W. Peter, H. Hess, H. R. Schöler, *Dev. Biol.* **166**, 259 (1994).
32. L. C. Stevens, D. S. Varnum, *Dev. Biol.* **37**, 369 (1974).
33. J. J. Eppig, K. Wigglesworth, D. S. Varnum, J. H. Nadeau, *Cancer Res.* **56**, 5047 (1996).
34. N. Hashimoto *et al.*, *Nature* **370**, 68 (1994).
35. C. Tilmann, B. Capel, *Recent Prog. Horm. Res.* **57**, 1 (2002).
36. J. S. Colvin, R. P. Green, J. Schmahl, B. Capel, D. M. Ornitz, *Cell* **104**, 875 (2001).
37. E. Simpson, D. Scott, P. Chandler, *Annu. Rev. Immunol.* **15**, 39 (1997).
38. S. Tanaka, T. Kunath, A. K. Hadjantonakis, A. Nagy, J. Rossant, *Science* **282**, 2072 (1998).
39. E. W. Carney, V. Prideaux, S. J. Lye, J. Rossant, *Mol. Reprod. Dev.* **34**, 357 (1993).
40. J. C. Chisholm, E. Houliston, *Development* **101**, 565 (1987).
41. M. Boiani, S. Eckardt, H. R. Schöler, K. J. McLaughlin, *Genes Dev.* **16**, 1209 (2002).

42. F. Guillemot, A. Nagy, A. Auerbach, J. Rossant, A. L. Joyner, *Nature* **371**, 333 (1994).
43. We thank J. Dean for generously providing the monoclonal ZP2 and ZP3 antibodies, P. Moens and B. Spyropoulos for SCP3/COR1 and SCP1/SYN1 antibodies, S. Eckardt and J. McLaughlin for providing a female ES cell line, T. Noce for providing the polyclonal Vasa antibody, E. Gonzales for helping with the immunocytochemistry, and A. Malapetsas for editing the manuscript. The Troma-1 hybridoma antibody, developed by P. Brulet and R. Kemler, was obtained from the Developmental Studies Hybridoma Bank developed under the auspices of the National Institute of Child Health and Human Development (of NIH) and maintained by the University of Iowa, Department of Biological Sciences. Supported, in part, by the Marion Dilley and David George Jones Funds, the Commonwealth and General Assembly of Pennsylvania, grant NIH 1RO1HD42011-01 (K.H., M.B., J.K., R.R., and H.S.), grant HD06274 (L.C., J.W., and J.S.), grant T32 HD07305 (J.W.), and grant 4434 (G.F.) from the Association pour la Recherche sur le Cancer.

Supporting Online Material

www.sciencemag.org/cgi/content/full/1083452/DC1
Materials and Methods
SOM Text
Figs. S1 and S2

12 February 2003; accepted 23 April 2003
Published online 1 May 2003;
10.1126/science.1083452
Include this information when citing this paper.

Keeping G Proteins at Bay: A Complex Between G Protein–Coupled Receptor Kinase 2 and Gβγ

David T. Lodowski,[1] Julie A. Pitcher,[2] W. Darrell Capel,[3] Robert J. Lefkowitz,[3] John J. G. Tesmer[1]*

The phosphorylation of heptahelical receptors by heterotrimeric guanine nucleotide–binding protein (G protein)–coupled receptor kinases (GRKs) is a universal regulatory mechanism that leads to desensitization of G protein signaling and to the activation of alternative signaling pathways. We determined the crystallographic structure of bovine GRK2 in complex with G protein $\beta_1\gamma_2$ subunits. Our results show how the three domains of GRK2—the RGS (regulator of G protein signaling) homology, protein kinase, and pleckstrin homology domains—integrate their respective activities and recruit the enzyme to the cell membrane in an orientation that not only facilitates receptor phosphorylation, but also allows for the simultaneous inhibition of signaling by Gα and Gβγ subunits.

G protein–coupled receptors (GPCRs) are integral membrane proteins that respond to specific extracellular signals by activating G proteins within the cell. They represent the largest class of receptors in the mammalian genome and play a fundamental role in the sensations of light, smell, and taste and in the regulation of heart rate, blood pressure, and glucose metabolism (*1*). For cells to remain responsive to their environment, activated GPCRs must be rapidly desensitized. The best characterized system for receptor desensitization is that of the GRKs and arrestins (*2, 3*). Activated GPCRs are first phosphorylated by GRKs and are then bound by molecules of arrestin, which block the binding of G proteins, target the receptors for clathrin-mediated endocytosis (*4*), and serve as adaptors that link receptors to other signaling pathways such as those of the mitogen-activated protein